

Evaluation of the neoclassical toroidal viscous torque in ASDEX Upgrade

A. F. Martitsch¹, S. V. Kasilov^{1,2}, W. Kernbichler¹, M. F. Heyn¹, E. Strumberger³, S. Fietz³,
W. Suttrop³, A. Kirk⁴, the ASDEX Upgrade Team³ and the EUROfusion MST1 Team *

¹ Fusion@ÖAW, Institut für Theoretische Physik - Computational Physics,
TU Graz, Petersgasse 16, A-8010 Graz, Austria

² Institute of Plasma Physics, National Science Center “Kharkov Institute of Physics and
Technology”, Akademicheskaya Str. 1, 61108 Kharkov, Ukraine

³ Max-Planck Institut für Plasmaphysik, D-85748 Garching, Germany

⁴ CCFE, Culham Science Centre, Abingdon, OX14 3DB, UK

Introduction

Non-axisymmetric non-resonant magnetic perturbations in a tokamak (e.g., toroidal field (TF) ripple, error fields, coils for ELM mitigation purposes) give rise to the so-called neoclassical toroidal viscous (NTV) torque, which can have a significant impact on the plasma rotation. The effect of the NTV torque on the plasma rotation has been observed in experiments [1]. For the evaluation of the NTV several analytical and semi-analytical approaches [2] are presently used, which make simplifying assumptions concerning geometry and collision operators. Numerical calculations of the NTV torque without such simplifications are presented here for the TF ripple and ELM mitigation coils in ASDEX Upgrade, and are compared to analytical models. The results are obtained from a quasilinear version of the code NEO-2, which is based on a numerical approach given in [3]. The only assumption is that the perturbations are small enough such that the particle motion within the perturbed flux surface is only weakly affected by the perturbation field (quasilinear approach). Since non-resonant magnetic perturbations are well described by the ideal MHD theory, the 3D equilibria of the ASDEX Upgrade discharges can be reconstructed using the code NEMEC [4]. These equilibria are used as an input for the upgraded code NEO-2.

Definitions

In Boozer coordinate system (r, ϑ, φ) with re-defined flux surface label [3], $\langle |\nabla r| \rangle = 1$ and metric determinant \sqrt{g} , the flux surface averaged NTV torque density T_φ^{NA} can be computed directly from the flux-force relation [2, 3],

$$T_\varphi^{\text{NA}} = -\frac{\sqrt{g}B^\vartheta}{c} \sum_\alpha e_\alpha \Gamma_\alpha^{\text{NA}}, \quad (1)$$

where $\sqrt{g}B^\vartheta = \partial \psi_{\text{pol}} / \partial r$ is the radial derivative of the poloidal flux and c , e_α and $\Gamma_\alpha^{\text{NA}}$ denote speed of light, charge and non-ambipolar particle flux density of species α , respectively. Here a co-variant notation is used for magnetic field, velocity and torque density components. The non-ambipolar particle fluxes are expressed through transport coefficients D_{ij}^{NA} and thermodynamic forces A_j ,

$$\Gamma_\alpha^{\text{NA}} = -n_\alpha (D_{11}^{\text{NA}} A_1 + D_{12}^{\text{NA}} A_2), \quad (2)$$

where n_α is α species density, and transport coefficients are evaluated by NEO-2. The thermodynamic forces are specified by

$$A_1 = \frac{1}{n_\alpha} \frac{\partial n_\alpha}{\partial r} - \frac{e_\alpha E_r}{T_\alpha} - \frac{3}{2T_\alpha} \frac{\partial T_\alpha}{\partial r}, \quad A_2 = \frac{1}{T_\alpha} \frac{\partial T_\alpha}{\partial r}, \quad (3)$$

* See <http://www.euro-fusionscipub.org/mst1>

where T_α and E_r are α species temperature and radial electric field, respectively. The radial electric field can be calculated from the toroidal rotation frequency of ions via the relation

$$V^\varphi = \frac{c}{\sqrt{g}B^\vartheta} \left(E_r - \frac{1}{e_i n_i} \frac{\partial(n_i T_i)}{\partial r} \right) + qV^\vartheta, \quad V^\vartheta = \frac{ckB_\varphi}{e_i \sqrt{g} \langle B^2 \rangle} \frac{\partial T_i}{\partial r}, \quad (4)$$

where q and $\langle \dots \rangle$ are safety factor and the neoclassical flux surface average, respectively. Here the coefficient $k = 5/2 - D_{32}/D_{31}$ is determined by the parallel ion flow obtained from the NEO-2 solution for the unperturbed, axisymmetric problem,

$$\langle V_{\parallel i} B \rangle = B_\varphi \left(V^\varphi - qV^\vartheta \right) + \frac{ckB_\varphi}{e_i \sqrt{g} B^\vartheta} \frac{\partial T_i}{\partial r} = -(D_{31}A_1 + D_{32}A_2). \quad (5)$$

Results

Evaluation of the NTV torque by NEO-2 and analytical models is performed here for the ASDEX Upgrade equilibrium #30835@3200ms provided by the code NEMEC. In Fig. 1 the experimentally measured profiles of density n_e , temperatures T_i and T_e , toroidal ion rotation frequency V^φ , and computed toroidal Mach number of the $\mathbf{E} \times \mathbf{B}$ rotation $M_t = cRE_r (v_T \sqrt{g} B^\vartheta)^{-1}$ as well as the safety factor for the corresponding shot are shown as functions of the normalized poloidal radius $\rho_{\text{pol}} = (\psi_{\text{pol}}/\psi_{\text{pol}}^a)^{1/2}$ where $\psi_{\text{pol}} = 0$ on the magnetic axis. In the pre-

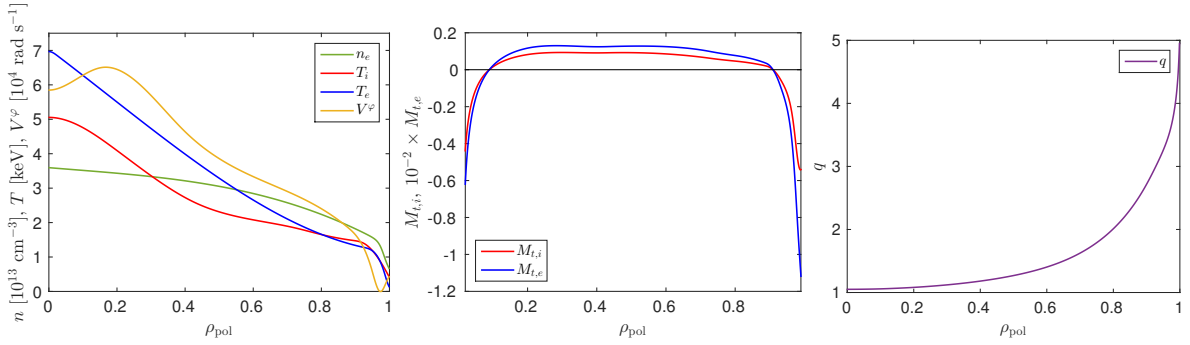


Figure 1: Radial profiles of density, temperatures, toroidal rotation frequency (left), toroidal Mach number (center) and safety factor (right) for ASDEX Upgrade shot #30835@3200ms.

sented modeling of the NTV torque non-resonant magnetic perturbations due to both, TF ripples (short-scale perturbation, $n=16$) and ELM mitigation coils (medium scale perturbation, $n=2,6$), are considered. For the TF ripple a comparison of NEO-2 results with analytical estimates of the torque density and integral torque,

$$T_\varphi^{\text{NA,int}} = \int_{V(\rho_{\text{pol}})} d^3r T_\varphi^{\text{NA}}, \quad (6)$$

where $V(\rho_{\text{pol}})$ is the volume limited by the flux surface with given ρ_{pol} , is shown in Fig. 2. It can be seen that the NTV torque acts in the direction opposite to the experimentally measured plasma rotation velocity and the integral torque is about -0.8 Nm. The NTV torque produced by TF ripples is mainly applied to ions and corresponds to the ripple-plateau regime [5] in most of the plasma volume. The analytical estimate, used here for comparison, can be obtained from a general expression for the particle flux in the ripple-plateau regime (Eq. (45) of Ref. [5]) by replacing in this derivation the simplified magnetic field with the more general form,

$$B(r, \vartheta, \varphi) = B_0(r, \vartheta) + B_n(r, \vartheta) \cos(n\varphi), \quad (7)$$

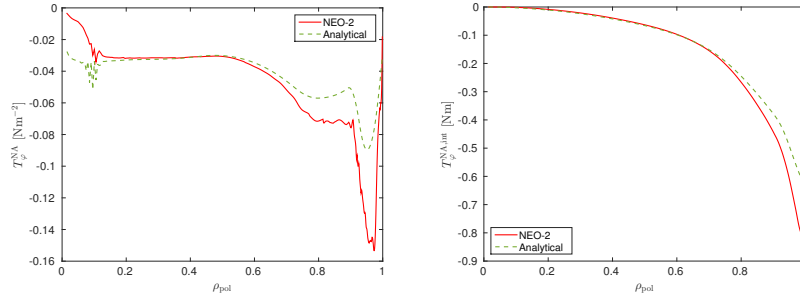


Figure 2: Radial profiles of the NTV torque density (left) and the integral torque (right) produced by the TF ripple.

where B_0 is the unperturbed magnetic field and B_n is the perturbation field amplitude. The non-ambipolar diffusion coefficients valid for a general tokamak geometry are then

$$D_{11}^{\text{NA}} = \frac{\sqrt{\pi}}{4} \frac{nm_i^2 c^2 v_T^3 B_0^2}{e_i^2 g(B_0^\vartheta)^2 B_0^\varphi} \left(\int_0^{2\pi} \frac{d\vartheta}{B_0} \right)^{-1} \int_0^{2\pi} \frac{d\vartheta}{B_0^3} \left(\frac{B_n}{B_0} \right)^2, \quad D_{12}^{\text{NA}} = 3D_{11}^{\text{NA}}, \quad (8)$$

where the notation is the same as in Ref. [3]. The difference in the integral torque between the NEO-2 result and the analytical estimate is less than 25%. In Fig. 3 NEO-2 results for the NTV torque density and integral torque produced by ELM mitigation coils are compared to the bounce-averaged model of Shaing [2, 3]. The integral torque produced by ELM mitigation coils is -0.5 Nm, and adds up to the torque produced by the TF ripple giving a total torque of -1.3 Nm. For the NTV torque, not only ions but also electrons make a significant contribution, which is in the direction of (positive) plasma rotation and which partly balances the negative ion torque. Note that the electron torque agrees by order of magnitude with the result of the asymptotical model [2]. The observed discrepancies can be attributed to the rather small aspect ratio where the analytical model of Shaing [2] can significantly deviate from accurate computations [3]. However, this is not the case for ions where NEO-2 results exceed the results of the asymptotical model [2] significantly. It should also be noted that the torque density profile exhibits distinctive substructures in the vicinity of resonant surfaces, which are indicated by the vertical lines. A rather peculiar point in this profile is the resonant surface $(m, n) = (6, 2)$ (light blue vertical line) which almost coincides with the zero of the electric field. The increased electron torque density around this point is due to the fact that for small values of the electric field $1/v$ transport is dominant in absence of resonant regimes. In order to determine relevant

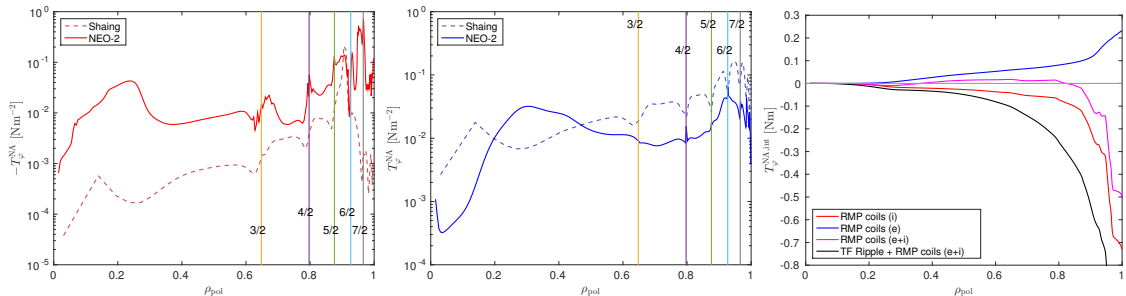


Figure 3: Ion (left) and electron (center) contribution of the ELM mitigation coils to the NTV torque density and the integral torque (right) computed by NEO-2 as functions of the normalized poloidal radius. Vertical lines indicate the positions of resonant surfaces with $q(\rho_{\text{pol}}) = m/n$, where m and n are the poloidal and toroidal mode numbers, respectively.

transport regimes, a scan of the diffusion coefficient D_{11}^{NA} over collisionality and otherwise the

same parameters as in the experimental profile has been performed at $\rho_{\text{pol}} = 0.5$, see Fig. 4. It is seen that electrons there are at the onset of $\nu - \sqrt{\nu}$ regime while the plateau like behavior of ion coefficient indicates the resonant diffusion regime. A drop of ion torque near the zero of the electric field corresponds to the reduced resonant contribution which at relatively low Mach numbers increases with M_t [6].

Discussion

The total value of the integral NTV torque for AUG shot #30835 as computed by NEO-2 is -1.3 Nm, which is less than the NBI torque value of +3.9 Nm. As it is known (see, e.g., Ref. [3]) the integral rotational moment is a conserved quantity and therefore missing balance between the NTV and NBI torques indicates the presence of other momentum sources. One obvious momentum source unaccounted here is the resonant torque [7], which is applied mainly to the electrons (and is positive) in resonant layers around rational flux surfaces where the ideal MHD theory is not valid. Other possible reasons for discrepancies could be the NTV torque produced by error fields and fields from eddy currents in the wall induced by intrinsic MHD modes, which are not taken into account in this computation and which can have both, resonant and non-resonant contributions. A further possible source is the momentum exchange through the plasma boundary. As it is known, particle and heat fluxes and also the toroidal momentum fluxes to the inner and outer divertor plates are generally not the same. In particular, this effect is responsible for the toroidal plasma spin up by gas puff [8]. Finally, losses of fast particles produced by NBI [9] can produce a significant negative torque. Thus, a study is of interest of the discharges where RMPs are absent and the rest volume sources of the momentum (NTV from TF ripple and error fields, and fast particle losses) are taken into account since the balance of these sources should be met with sources at the edge.

Acknowledgement

This work has been carried out within the framework of the EUROfusion Consortium and has received funding from the Euratom research and training programme 2014-2018 under grant agreement No 633053. The views and opinions expressed herein do not necessarily reflect those of the European Commission. The authors gratefully acknowledge support from NAWI Graz.

References

- [1] W. Zhu *et al*, Phys. Rev. Lett. **96**, 225002 (2006); A. M. Garofalo *et al*, Phys. Plasmas **16**, 056119 (2009); Y. Sun *et al*, Nucl. Fusion **52**, 083007 (2012).
- [2] K. C. Shaing *et al*, Nucl. Fusion, **50**, 025022 (2010); J. Park *et al*, Phys. Rev. Lett. **102**, 065002 (2009); Y. Sun *et al*, Phys. Rev. Lett. **105**, 145002 (2010).
- [3] S. V. Kasilov *et al*, Phys. Plasmas **21**, 092506 (2014).
- [4] S. P. Hirshman *et al*, Comput. Phys. Commun. **43**(1), 143-155 (1986).
- [5] A. H. Boozer, Phys. Fluids, **23**, 2283, 1980.
- [6] C. G. Albert *et al*, this conference, P1.183.
- [7] M. F. Heyn *et al*, Nucl. Fusion **54**, 064005 (2014).
- [8] V. Rozhansky *et al*, J. Nucl. Mater. **291**, 337-339 (2005).
- [9] T. Kurki-Suonio *et al*, Plasma Phys. Contr. Fusion **42**, 277-282 (2000).

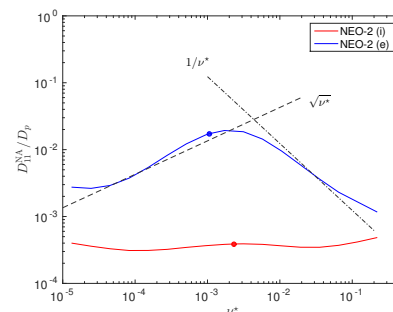


Figure 4: Diffusion coefficient normalized by the plateau diffusion coefficient $D_p = \pi q v_T \rho_L^2 (16R)^{-1}$ for $\rho_{\text{pol}} = 0.5$ as a function of the collisionality parameter $\nu^* = 2\nu q R v_T^{-1}$. Actual collisionalities for the poloidal radius are shown by filled circles. Note that the normalizing plateau diffusion coefficient is by a square-root of mass ratio smaller for electrons than for ions.